Accepted for publication in the Astrophysical Journal, July 16, 2007
Preprint typeset using LaTeX style emulateapj v. 10/09/06

arXiv:0704.0792v2 [astro-ph] 17 Jul 2007

THE RELATIONSHIP BETWEEN MOLECULAR GAS TRACERS AND KENNICUTT-SCHMIDT LAWS

Mark R. Krumholz[1] and Todd A. Thompson[2]
Department of Astrophysical Sciences, Princeton University, Princeton, NJ 08544
Accepted for publication in the Astrophysical Journal, July 16, 2007

ABSTRACT

We provide a model for how Kennicutt-Schmidt (KS) laws, which describe the correlation between star formation rate and gas surface or volume density, depend on the molecular line chosen to trace the gas. We show that, for lines that can be excited at low temperatures, the KS law depends on how the line critical density compares to the median density in a galaxy's star-forming molecular clouds. High critical density lines trace regions with similar physical properties across galaxy types, and this produces a linear correlation between line luminosity and star formation rate. Low critical density lines probe regions whose properties vary across galaxies, leading to a star formation rate that varies superlinearly with line luminosity. We show that a simple model in which molecular clouds are treated as isothermal and homogenous can quantitatively reproduce the observed correlations between galactic luminosities in far infrared and in the CO($1 \rightarrow 0$) and HCN($1 \rightarrow 0$) lines, and naturally explains why these correlations have different slopes. We predict that IR-line luminosity correlations should change slope for galaxies in which the median density is close to the line critical density. This prediction may be tested by observations of lines such as $HCO^+(1 \rightarrow 0)$ with intermediate critical densities, or by HCN($1 \rightarrow 0$) observations of intensely star-forming high redshift galaxies with very high densities. Recent observations by Gao et al. hint at just such a change in slope. We argue that deviations from linearity in the HCN($1 \rightarrow 0$)$-$IR correlation at high luminosity are consistent with the assumption of a constant star formation efficiency.

Subject headings: ISM: clouds — ISM: molecules — stars: formation — galaxies: ISM — radio lines: ISM

1. INTRODUCTION

Schmidt (1959, 1963) first proposed that the rate at which a gas forms stars might follow a simple power law correlation of the form $\dot{\rho}_* \propto \rho_g^N$, where $\dot{\rho}_*$ is the star formation rate per unit volume, ρ_g is the gas density, and N is generally taken to be in the range $1-2$. In the decades since, observations have revealed two strong correlations that appear to be evidence for this hypothesis. First, galaxy surveys reveal that the infrared luminosity of a galaxy, which traces the star formation rate, varies with its luminosity in the CO($1 \rightarrow 0$) line, which traces the total mass of molecular gas, as $L_{\rm FIR} \propto L_{\rm CO}^{1.4-1.6}$ (Gao & Solomon 2004a,b; Greve et al. 2005; Riechers et al. 2006a). Kennicutt (1998a,b) identified the closely-related correlation between gas surface density Σ_g and star formation rate surface density $\dot{\Sigma}_*$, $\dot{\Sigma}_* \propto \Sigma_g^{1.4\pm0.15}$, a relation that has come to be known as the Kennicutt Law. Since over the bulk of the dynamic range of Kennicutt's data galaxies are predominantly molecular, this is effectively a correlation between molecular gas, as traced by CO($1 \rightarrow 0$) line emission, and star formation. Spatially resolved observations of galaxies confirm that, at least for molecule-rich galaxies where resolved CO($1 \rightarrow 0$) observations are possible, star formation is more closely coupled with gas traced by CO($1 \rightarrow 0$) than with atomic gas (Wong & Blitz 2002; Heyer et al. 2004; Komugi et al. 2005; Kennicutt et al. 2007)

Second, Gao & Solomon (2004a,b) find that there is a strong correlation between the IR luminosity of galaxies and emission in the HCN($1 \rightarrow 0$) line, which measures the mass at densities significantly greater than that probed by CO($1 \rightarrow 0$). However, they find that their correlation, which covers nearly three decades in total galactic star formation rate, is linear: $L_{\rm FIR} \propto L_{\rm HCN}$. Wu et al. (2005) show that this correlation extends down to individual star-forming clumps of gas in the Milky Way, provided that their infrared luminosities are $\gtrsim 10^{4.5}\,L_\odot$. Interestingly, however, Gao et al. (2007) find a deviation from linearity in the IR-HCN correlation for a sample of intensely star-forming high redshift galaxies. These sources show small but significant excesses of infrared emission for their observed HCN emission.

The difference in power law indices between the $L_{\rm FIR} - L_{\rm CO}$ and $L_{\rm FIR} - L_{\rm HCN}$ correlations is statistically significant, and, on its face, puzzling. An index near $N = 1.5$ seems natural if one supposes that a roughly constant fraction of the gas present in molecular clouds will be converted into stars each free-fall time. In this case one expects $\dot{\rho}_* \propto \rho_g^{1.5}$ (Madore 1977; Elmegreen 1994). If gas scale heights do not vary strongly from galaxy to galaxy, this implies $\dot{\Sigma}_* \propto \Sigma_g^{1.5}$ as well, which is consistent with the observed Kennicutt law. More generally, since the dynamical timescale in a marginally Toomre-stable ($Q \approx 1$; see Martin & Kennicutt 2001) galactic disk is of order $\Omega^{-1} \propto (G\rho_g)^{-1/2}$, where Ω is the angular frequency of the disk, an index close to $N = 1.5$ is expected if star formation is regulated by any phenomenon that converts a fixed fraction of the gas into stars on this time scale (Elmegreen 2002).

On the other hand, Wu et al. (2005) suggest a simple interpretation of the linear IR-HCN correlation. They ar-

Electronic address: krumholz@astro.princeton.edu, thomp@astro.princeton.edu
[1] Hubble Fellow
[2] Lyman Spitzer Jr. Fellow

gue that the individual HCN-emitting molecular clumps that they identify in the Milky Way represent a fundamental unit of star formation. The linear correlation between star formation rate and HCN luminosity across galaxies arises because a measurement of the HCN luminosity for a galaxy simply counts the number of such structures present within it, each of which forms stars at some roughly fixed rate regardless of its galactic environment. However, in this interpretation it is unclear why the structures traced by HCN($1 \rightarrow 0$) emission should form stars at the same rate in any galaxy. After all, one could equally well argue that molecular clouds traced by CO($1 \rightarrow 0$) are fundamental units of star formation, but the non-linear IR-CO correlation clearly shows that these objects do not form stars at a fixed rate per unit mass. Moreover, the evidence presented by Gao et al. (2007) that the linear IR-HCN correlation varies in extremely luminous high redshift galaxies suggests that the relationship between HCN emission and star-formation may be somewhat more complex.

In this paper we attempt to explain the origin of the difference in slope between the CO and HCN correlations with star formation rate, and more generally to give a theoretical framework for understanding how correlations between star formation rate and line luminosity, which we generically refer to as Kennicutt-Schmidt (KS) laws, depend on the tracer used to define them. Our central argument is conceptually quite simple, and in some sense represents a combination of the intuitive arguments for CO and HCN given above.

Consider an observation of a galaxy in a molecular tracer with critical density $n_{\rm crit}$, which essentially measures the mass of gas at densities of $n_{\rm crit}$ or more, i.e. the gas that is dense enough for that particular transition to be excited. In galaxies where the median density of the molecular gas is significantly larger than $n_{\rm crit}$, this means that the observation will detect the majority of the gas, and the bulk of the emission will come from gas whose density is near the median density. Since the gas density will vary from galaxy to galaxy, the star formation rate per unit gas mass will vary as roughly $\rho_g^{1.5}$, with one factor of ρ_g coming from the amount of gas available for star formation, and an additional factor of $\rho_g^{0.5}$ coming from the dependence of the free-fall or dynamical time on the density.

On the other hand, in galaxies where the median gas density is small compared to the critical density for the chosen transition, observations will pick out only high density peaks. Since the density in these peaks is set by $n_{\rm crit}$, and not by the conditions in the galaxy, these peaks are at essentially the same density in any galaxy where they are observed, and the corresponding free-fall times in these regions are constant as well. As a result, the star formation rate per unit mass of gas traced by that line is approximately the same in every galaxy, because the corresponding free-fall time is the same in every galaxy.

In the rest of this paper, we give a quantitative version of this intuitive argument, and then discuss its consequences. In § 2 we develop a simple formalism to compute the star formation rate and the molecular line luminosity of galaxies, and in § 3 we use this formalism to predict the correlation between star formation rate and luminosity. We show that our predictions provide a very good fit for a variety of observations, and make predictions for future observations. We discuss the implications of our work and its limitations in § 4, and summarize our conclusions is § 5.

2. STAR FORMATION RATES AND LINE LUMINOSITIES

2.1. *Cloud Properties*

Consider a galaxy in which the star-forming molecular clouds have a volume-averaged mean molecular hydrogen number density $\overline{n} = \overline{\rho}_g/\mu_{H_2}$, where $\overline{\rho}_g$ is the volume-averaged mass density of the molecular clouds in the galaxy and $\mu_{H_2} = 3.9 \times 10^{-24}$ g is the mean mass per hydrogen molecule for a gas of standard cosmic composition. Observations indicate that $\overline{n}$ varies by two to three decades over the galaxies for which the Kennicutt and Gao & Solomon correlations are measured, from $\overline{n} \approx 50$ cm^{-3} in normal spirals like the Milky Way (McKee 1999) up to $\overline{n} \approx 10^4$ cm^{-3} in the strongest starburst systems in the local universe (e.g. Downes & Solomon 1998). There is strong evidence that densities in molecular clouds follow a lognormal probability distribution function (PDF; see reviews by Mac Low & Klessen 2004 and Elmegreen & Scalo 2004)

$$\frac{dp}{d\ln x} = \frac{1}{\sqrt{2\pi\sigma^2}} \exp\left[-\frac{(\ln x - \overline{\ln x})^2}{2\sigma^2}\right], \qquad (1)$$

where $x = n/\overline{n}$ is the molecular hydrogen number density n relative to the average density, σ is the width of the lognormal, and $\overline{\ln x} = -\sigma^2/2$. For this distribution the median density is $n_{\rm med} = \overline{n}\exp(\sigma^2/2)$. Numerical experiments show that for supersonic isothermal turbulence $\sigma^2 \approx \ln\left(1 + 3\mathcal{M}^2/4\right)$, where $\mathcal{M}$ is the 1D Mach number of the turbulence (Nordlund & Padoan 1999; Ostriker et al. 1999; Padoan & Nordlund 2002). Mach numbers in star-forming molecular clouds range from $\mathcal{M} \sim 30$ (McKee 1999) in normal spirals to $\mathcal{M} \sim 100$ in strong starbursts (Downes & Solomon 1998), implying that median densities in molecular clouds range from $\sim 10^3$ cm^{-3} in normal spirals to $\sim 10^6$ cm^{-3} in starbursts. Star forming clouds within a galaxy are approximately isothermal, except very near strong sources of stellar radiation, so we assume a fixed temperature T for the clouds. Observationally, T ranges from roughly 10 K in normal spirals (McKee 1999) up to as much about 50 K in strong starbursts (Downes & Solomon 1998; Gao & Solomon 2004b).

2.2. *Star Formation Rates*

First let us ask how quickly stars form in such a medium. Krumholz & McKee (2005) give a model for star formation regulated by supersonic turbulence in which a population of molecular clouds of total mass $M_{\rm cl}$ form stars at a rate $\dot{M}_* = {\rm SFR_{ff}} M_{\rm cl}/t_{\rm ff}(\overline{n})$, where $t_{\rm ff}(\overline{n})$ is the free-fall time evaluated at the mean density and ${\rm SFR_{ff}}$ is a number of order 10^{-2} that depends weakly on $\mathcal{M}$. We therefore estimate the star formation rate per unit volume as a function of the mean density given by

$$\dot{\rho}_* \approx {\rm SFR_{ff}} \sqrt{\frac{32 G \mu_{H_2}^3 \overline{n}^3}{3\pi}}. \qquad (2)$$

We adopt the Krumholz & McKee result ${\rm SFR_{ff}} \approx 0.014(\mathcal{M}/100)^{-0.32}$ for clouds with a fiducial virial ratio of $\alpha_{\rm vir} = 1.3$.

Alternately, Krumholz & Tan (2007) point out that observed correlations between the star formation rate and the luminosity in different density tracers imply that over a $3-4$ decade range in density n,

$$\dot{M}_* \approx 10^{-2} \frac{M_{\rm cl}(>n)}{t_{\rm ff}(n)}, \quad (3)$$

where $M_{\rm cl}(>n)$ is the mass of gas with a density of n or higher, and $M_{\rm cl} = M_{\rm cl}(>0)$. For a given choice of n this provides an alternative estimate of the star formation rate which is purely empirical, and independent of any particular theoretical model. However, the difference between the star formation rates predicted by (2) and (3) is small. For gas with a lognormal PDF,

$$M_{\rm cl}(>n) = \frac{M_{\rm cl}}{2}\left(1+\mathrm{erf}\left[\frac{-2\ln x+\sigma^2}{2^{3/2}\sigma}\right]\right), \quad (4)$$

and using this to evaluate equation (3) indicates that, for Mach numbers in the observed range, the two prescriptions (2) and (3) give about the same star formation rate over a very broad range in x. For example, at $\mathcal{M}=30$ the two estimates agree to within a factor of 3 for densities in the range $0.2 < x < 4\times10^4$. Given the scatter inherent in observational estimates of the star formation rate, a factor of 3 difference is not particularly significant, so it matters little which prescription we adopt. In practice, we will use equation (2).

2.3. *Line Luminosities*

Now we must compute the luminosity of molecular line emission from the galaxy. Even for a cloud that is not in local thermodynamic equilibrium (LTE), for optically thin emission this calculation is straightforward. However, the molecular lines used most often in galaxy surveys are generally optically thick. To handle the effect of finite optical depth on molecule level populations and line luminosities, we adopt an escape probability approximation and treat clouds as homogeneous spheres. This is not fully consistent with our assumption that clouds have lognormal density PDFs, since the escape probability formalism assumes a uniform level population throughout the cloud, and the essence of our argument in this paper turns on how the level population varies with density. However, this approach gives us an approximate way of incorporating the optical thickness of star-forming clouds into our model, the only alternative to which for turbulent media is full numerical simulation (e.g. Juvela et al. 2001). We therefore proceed by treating clouds as homogeneous in order to determine their escape probabilities, and we then relax the assumption of homogeneity, while keeping the escape probabilities fixed, in order to determine level populations and cloud luminosities as a function of density.

Consider a cloud of radius R in statistical equilibrium but not necessarily in LTE. In the escape probability approximation, the fraction f_i of molecules of species S in state i is given implicitly by the linear system

$$\sum_j \left(n q_{ji} + \beta_{ji} A_{ji}\right) f_j = \left[\sum_j \left(n q_{ij} + \beta_{ij} A_{ij}\right)\right] f_i \quad (5)$$

$$\sum_i f_i = 1, \quad (6)$$

where q_{ij} is the collision rate for transitions from state i to state j, A_{ij} is the Einstein spontaneous emission coefficient for this transition, β_{ij} is the cloud-averaged escape probability for photons emitted in this transition, the sums are over all quantum states, and we understand that $A_{ij}=0$ for $i \le j$ and $q_{ij}=0$ for $i=j$.

Equations (5) and (6) allow us to compute the level populations f_i for given values of β_{ij}. To completely specify the system, we must add an additional consistency condition relating the values of β_{ij} to the level populations. For a homogeneous spherical cloud, the escape probability for a given line is related to the optical depth from the center to the edge of the cloud τ_{ij} by (B. Draine, 2007, private communication)

$$\beta_{ij} \approx \frac{1}{1+0.5\tau_{ij}}, \quad (7)$$

where τ_{ij} is computed at the central frequency of the line. In turn, the optical depth is related to the level populations by

$$\tau_{ij} = \frac{g_j}{g_j}\frac{A_{ij}\lambda_{ij}^3}{4(2\pi)^{3/2}\mathcal{M}c_s}\overline{n}X(S)f_j R\left(1-\frac{f_i g_j}{f_j g_i}\right), \quad (8)$$

where λ_{ij} is the wavelength of transition $i \rightarrow j$, g_i and g_j are the statistical weights of states i and j, c_s is the isothermal sound speed of the gas, and $X(S)$ is the abundance of molecules of species S. Note that this equation implicitly assumes that the cloud has a uniform Maxwellian velocity distribution with 1D dispersion $\mathcal{M}c_s$, consistent with our treatment of the clouds as homogeneous spheres. One additional complication is that we do not directly know cloud radii for most external galaxies, where observations cannot resolve individual molecular clouds. However, we often can diagnose the optical depths of transitions by comparing line ratios of molecular isotopomers of different abundances. We therefore take τ_{10}, the optical depth of the transition between the first excited state and the ground state, as known. For a given level population this fixes the value of R.

We solve equations (5)–(8) using Newton-Raphson iteration. In this procedure, we guess an initial set of escape probabilities β_{ij}, and solve the linear system (5) and (6) to find the corresponding initial level populations f_i. We then compute the optical depths τ_{ij} from equation (8). The guessed escape probabilities β_{ij} and the corresponding optical depths τ_{ij} generally will not satisfy the consistency condition (7), so we then iterate over β_{ij} values using a Newton-Raphson approach, seeking β_{ij} for which the level populations give optical depths τ_{ij} such that all elements of the matrix $\beta_{ij} - 1/(1+0.5\tau_{ij})$ are equal to zero within some specified tolerance. We use the LTE level populations and escape probabilities for our initial guess, so that the iteration converges rapidly when the system is close to LTE.

Once we have determined the escape probabilities β_{ij}, we compute the luminosity by holding the β_{ij} values fixed but allowing the level populations to vary with density, then integrating over the PDF. Thus, the total luminosity per unit volume in a particular line is

$$L_{ij} = X(S)\beta_{ij}A_{ij}h\nu_{ij}\int_{-\infty}^{\infty} f_i n \frac{dp}{d\ln x} d\ln x, \quad (9)$$

TABLE 1
Model Parameters

Parameter	Normal galaxy	Intermediate	Starburst	Reference
T	10	20	50	1–4
$\mathcal{M}$	30	50	80	1–4
X(CO)	2×10^{-4}	4×10^{-4}	8×10^{-4}	5
X(HCO^+)	2×10^{-9}	4×10^{-9}	8×10^{-9}	6, 7
X(HCN)	1×10^{-8}	2×10^{-8}	4×10^{-8}	6–8
$\tau_{CO(1\rightarrow0)}$	10	20	40	9
$\tau_{HCO^+(1\rightarrow0)}$	0.5	1.0	2.0	6, 7
$\tau_{HCN(1\rightarrow0)}$	0.5	1.0	2.0	6, 7
OPR	0.25	0.25	0.25	10

Note. — OPR = H_2 ortho- to para-ratio. References: 1 – Solomon et al. (1987), 2 – Gao & Solomon (2004b), 3 – Downes & Solomon (1998), 4 – Wu et al. (2005), 5 – Black (2000), 6 – Nguyen et al. (1992), 7 – Wild et al. (1992), 8 – Lahuis & van Dishoeck (2000), 9 – Combes (1991), 10 – Neufeld et al. (2006)

where ν_{ij} is the line frequency, f_i is an implicit function of n given by the solution to equations (5) and (6), and we assume that the abundance $X(S)$ is independent of n. The line luminosity per unit mass is $L_{ij}/(\mu_{H_2}\overline{n})$.

An IDL code that implements this calculation is available for public download from http://www.astro.princeton.edu/∼krumholz/ astronomy.html.

3. CORRELATIONS AND KENNICUTT-SCHMIDT LAWS

3.1. *Lines and Parameters*

Using the formalism of § 2, we can now predict the correlation between the star formation rate and the luminosity of a galaxy in molecular lines. We make these predictions for three representative molecular lines: CO($1 \rightarrow 0$), $HCO^+(1 \rightarrow 0)$, and HCN($1 \rightarrow 0$). For the first and last of these transitions, there are extensive observational surveys. We select $HCO^+(1 \rightarrow 0)$ in addition to these two because there is some observational data for it, and because its critical density of $n_{\rm crit} = \beta_{\rm HCO+} 4.6 \times 10^4$ cm^{-3} makes it intermediate between CO($1 \rightarrow 0$), with $n_{\rm crit} = \beta_{\rm CO} 560$ cm^{-3}, and HCN($1 \rightarrow 0$), with $n_{\rm crit} = \beta_{\rm HCN} 2.8 \times 10^5$ cm^{-3}.[3] Here β_S is the escape probability for the $1 \rightarrow 0$ transition of species S. These critical densities are for $T = 20$ K. All molecular data are taken from the Leiden Atomic and Molecular Database[4] (Schöier et al. 2005).

We make our calculations for three sets of fiducial parameters which we summarize in Table 1. The three sets correspond roughly to typical conditions in normal disk galaxies like the Milky Way, to starburst galaxies like Arp 220, and to a case intermediate between the two. We have selected parameters for each case to roughly model the systematic variation of ISM parameters as one moves from normal disk galaxies to starbursts. Thus, we vary the ISM temperature from $10 - 50$ K and the molecular cloud Mach number from $30 - 80$ as we move from Milky Way-like molecular clouds to temperatures and Mach numbers typical of starbursts (e.g. Downes & Solomon 1998). Similarly, starbursts, which preferentially occur at galactic centers, have systematically larger metallicities than galaxies like the Milky Way (e.g. Zaritsky et al. 1994; Yao et al. 2003; Netzer et al. 2005). To explore this effect, we use abundances and $1 \rightarrow 0$ optical depths are twice and four times as large for our intermediate and starburst models, respectively, as for our normal galaxy model.

[3] Note that our critical density for HCN($1 \rightarrow 0$) is somewhat larger than the value quoted by Gao & Solomon (2004a,b), probably because their calculation is based on somewhat different assumptions about how to extrapolate from calculated rate coefficients for HCN collisions with He to collisions with H_2. See Schöier et al. (2005) for details.

[4] http://www.strw.leidenuniv.nl/∼moldata/

3.2. *Kennicutt-Schmidt Laws*

We first plot, in Figure 1, the quantities $L^{-1}[dL(< n)/d\ln n]$ (*solid lines*) and $M^{-1}[dM(< n)/d\ln n]$ (*dotted lines*) as a function of density n for galaxies with mean densities $\overline{n} = 10^2$, 10^3, and 10^4 cm^{-3}, for the tracers CO($1 \rightarrow 0$), $HCO^+(1 \rightarrow 0)$, and HCN($1 \rightarrow 0$), and for the Mach number and temperature corresponding to our intermediate case in Table 1. Here $L(< n)$ and $M(< n)$ are the luminosity and mass per unit volume contributed by gas of density n or less, i.e. $L(< n) = X(S)\beta_{ij}A_{ij}h\nu_{ij}\int_{-\infty}^{\ln n} f_i n(dp/d\ln n)d\ln n$, $M(< n) = \int_{-\infty}^{\ln n} \mu_{H_2} n(dp/d\ln n)d\ln n$, $L = L(< \infty)$, and $M = M(< \infty)$. Physically, $L^{-1}[dL(< n)/d\ln n]$ and $M^{-1}[dM(< n)/d\ln n]$ represent the fractional contribution to the total line luminosity and the total mass that comes from each unit interval in the logarithm of density. The plot shows what density range provides the dominant contribution to the line luminosity in different lines and for galaxies of differing mean densities, and how the gas contributing light compares to the gas contributing mass. Because the mass distribution is entirely specified by $\overline{n}$ and $\mathcal{M}$, the dotted lines are the same in each of the three panels. Additionally, because of our choice $\mathcal{M} = 50$ (Table 1), the median density (the density corresponding to the peak in $M^{-1}[dM(< n)/d\ln n]$) is $n_{\rm med} \approx 43\,\overline{n}$. In each panel, the critical density for each molecule is identified by a vertical dashed line.

The top panel clearly shows that for the CO line, the light and the mass track one another very closely, even at the lowest densities. Thus, because $n_{\rm med} > n_{\rm crit}$, the solid lines move in lock-step with the dashed lines as $\overline{n}$ increases. In contrast, for HCN most of the luminosity comes from densities near the critical density regardless of the mass distribution. For the lowest $\overline{n}$ this means that the line luminosity is entirely dominated by the high density tail of the mass distribution. As the median density

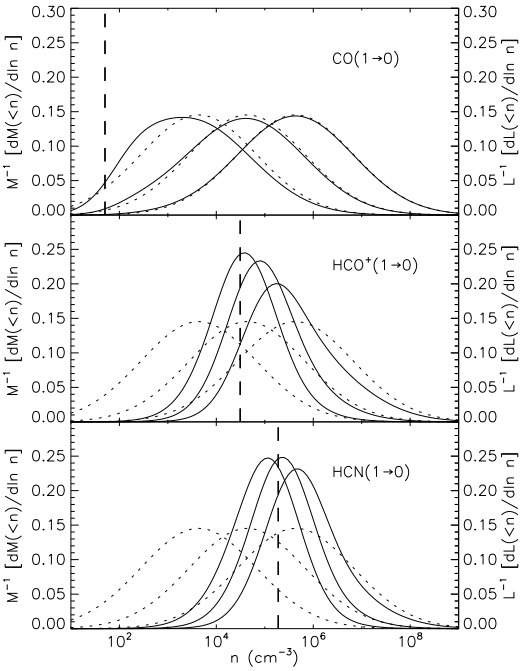

FIG. 1.— Fractional contribution to the total luminosity $L^{-1}[dL(<n)/d\ln n]$ (*solid lines*) and mass $M^{-1}[dM(<n)/d\ln n]$ (*dotted lines*) versus density n for the lines CO($1 \rightarrow 0$) (*top panel*), HCO$^+$($1 \rightarrow 0$) (*middle panel*), and HCN($1 \rightarrow 0$) (*bottom panel*). The three curves show the cases $\overline{n} = 10^2$ cm^{-3}, 10^3 cm^{-3}, and 10^4 cm^{-3}, from leftmost to rightmost. We also show the critical density of each molecule, corrected for radiative trapping (*dashed vertical lines*). These calculations use the parameters for the intermediate case listed in Table 1.

$n_{\rm med}$ varies by a factor of 100 (from $4.3 \times 10^3 - 4.3 \times 10^5$ cm^{-3}), the peak of $L^{-1}[dL(<n)/d\ln n]$ moves by just a factor of a few in n. The HCO$^+$ line is intermediate between CO and HCN. For $\overline{n} = 10^2$ cm^{-3} and 10^3 cm^{-3}, $n_{\rm med} \lesssim n_{\rm crit}$, and as with HCN most of the emission comes from near the critical density. For $\overline{n} = 10^4$ cm^{-3}, $n_{\rm med} > n_{\rm crit}$, and the light starts to follow the mass, in a pattern similar to that for CO. Although Figure 1 shows only the intermediate case, the normal galaxy and starburst cases give qualitatively identical results. This confirms the intuitive argument given in § 1: *high critical density transitions trace regions of similar density in every galaxy, while low critical density transitions trace regions whose density is close to the median density.*

Now consider how the luminosity in a given line correlates with the star formation rate in galaxies of varying mean densities. For a given $\overline{n}$, we can compute the volume density of star formation from equation (2) and the line luminosity density from (9). To facilitate comparison with observations, rather than considering the total line luminosity, we use the quantity L' (Solomon et al. 1997), which is related to the luminosity L by

$$L' = \frac{c^2}{8\pi k_B \nu^2} L, \tag{10}$$

converted to the units K km s^{-1} pc^2.

Similarly, we can estimate the far infrared luminosity from the star formation rate. There is a tight correlation between far-IR emission and star formation, particularly for dense, dusty galaxies like those that make up most of the dynamic range of the Kennicutt (1998a) sample. To the extent that most or all of the light from young stars is re-processed by dust before escaping the galaxy, the bolometric luminosity integrated over the wavelength range $8 - 1000$ μm, which we define as $L_{\rm FIR}$, simply provides a calorimetric measurement of the total energy output by young stars, and is therefore an excellent tracer of recent star formation (Sanders & Mirabel 1996; Rowan-Robinson et al. 1997; Kennicutt 1998a,b; Hirashita et al. 2003; Bell 2003; Iglesias-Páramo et al. 2006). We therefore estimate the FIR luminosity from the star formation rate via

$$L_{\rm FIR} = \epsilon \dot{M}_* c^2, \tag{11}$$

where ϵ is an IMF-dependent constant. For consistency with Kennicutt (1998a,b), we take $\epsilon = 3.8 \times 10^{-4}$. To be precise and to facilitate comparison with observations, we adopt the Sanders & Mirabel (1996) definition of $L_{\rm FIR}$ as a weighted sum of the luminosity in the 60 and 100 μm IRAS bands. This definition of the infrared luminosity generically underestimates the total infrared luminosity $[8 - 1000]\mu$m by a factor of $1.5 - 2$ (Calzetti et al. 2000; Dale et al. 2001; Bell 2003). However, we use the ϵ value appropriate for $L_{\rm FIR}$ rather than for the total IR luminosity because some of the observations to which we wish to compare our model (see § 3.3) provide only $L_{\rm FIR}$. Note that this choice for the connection between the star formation rate and the infrared luminosity is not fully consistent with our choice of the gas temperature for the three sets of parameters — normal, intermediate, and starburst — listed in Table 1, an issue we discuss in more detail in § 4.3.

We plot the ratio of star formation rate to line luminosity, and infrared luminosity to line luminosity, as a function of $\overline{n}$ in Figure 2. First consider the top panel, which shows all three lines computed for the intermediate case. This again confirms our intuitive argument. Since the luminosity per unit volume in the CO line is roughly proportional to the mass density, and the star formation rate / IR luminosity is proportional to mass density to the 1.5 power, the ratios $\dot{M}_*/L'$ and $L_{\rm FIR}/L'$ vary roughly as $\overline{n}^{0.5}$. A powerlaw fit to the data over the range shown in Figure 2 gives an index of 0.57. In contrast, the ratio of star formation density to HCN luminosity density is nearly constant for galaxies with $\overline{n} < 10^3$ cm^{-3}, and varies quite weakly with $\overline{n}$ up to densities of 10^4 cm^{-3}, values found in the densest starbursts. A powerlaw fit from 10 cm^{-3} to 10^4 cm^{-3} gives an index of 0.17; from 10 cm^{-3} and 10^3 cm^{-3}, the best fit powerlaw index is 0.08. As in Figure 1, the slope of the $\dot{M}_*/L'$ curve for HCO$^+$ represents an intermediate case, with a roughly constant ratio of $\dot{M}_*/L'$ and $L_{\rm FIR}/L'$ at low $\overline{n}$, rising to a slope comparable to that for CO at high values of $\overline{n}$.

Now consider the bottom three panels in Figure 2. Each panel shows the ratio of star formation rate and infrared luminosity to line luminosity for a single line, computed for each of the three galaxy models. The most important point to take from these plots is that the choice of galaxy model has little effect in most cases. The largest differences are for HCN, where at $\overline{n} = 10$ cm^{-3} the IR to line ratio predicted for the intermediate case differs from the normal galaxy case by a factor of 6.1, and from the starburst case by a factor of 4.1. This variation comes

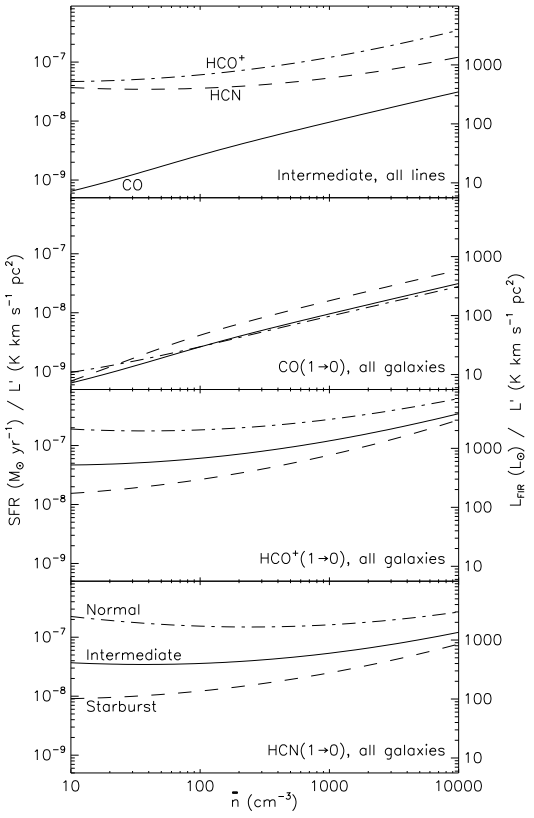

FIG. 2.— Ratio of star formation rate or infrared luminosity to line luminosity, as a function of mean density $\overline{n}$. In the top panel we show the lines CO($1 \rightarrow 0$) (*solid line*), $HCO^+(1 \rightarrow 0)$ (*dot-dashed line*), and HCN($1 \rightarrow 0$) (*dashed line*) for the intermediate case in Table 1. In the next three panels we show the CO($1 \rightarrow 0$), $HCO^+(1 \rightarrow 0)$, and HCN($1 \rightarrow 0$) lines for the normal galaxy case (*dot-dashed line*), intermediate case (*solid line*), and starburst case (*dashed line*).

primarily from changes in the Mach number and the optical depth between models. The higher Mach number of the starburst model significantly increases the amount of mass in the high overdensity tail of the probability distribution, while the higher optical depth lowers the effective critical density. Both of these effect increase the amount of mass dense enough to emit in HCN($1 \rightarrow 0$) and reduce $\dot{M}_*/L'$. At higher mean densities these effects become less important and the models converge, so that by $\overline{n} = 10^4$ cm^{-3} the range in $\dot{M}_*/L'$ from the normal to the starburst case is only a factor of 3.5.

Most importantly, our central conclusion that $\dot{M}_*/L'_{\rm HCN}$ is roughly constant across galaxies, while $\dot{M}_*/L'_{\rm CO}$ rises as roughly $[L'_{\rm CO}]^{0.5}$, still holds when we consider how conditions vary across galaxies. Galaxies with low mean densities $\overline{n}$ are generally closest to the normal galaxy case, while those with high mean densities should be closest to the starburst case, and this systematic variation in galaxy properties with $\overline{n}$ still leaves $\dot{M}_*/L'$ relatively flat for HCN, and varying with a slope close to 0.5 for CO. From the normal galaxy case at $\overline{n} = 10$ cm^{-3} to the starburst case at $\overline{n} = 10^4$ cm^{-3}, the value of $\dot{M}_*/L'$ varies by more than a factor of 50 for the CO($1 \rightarrow 0$), but by less than a factor of 3 for the HCN($1 \rightarrow 0$).

3.3. *Comparison with Observations*

The calculations illustrated in Figure 2 demonstrate the basic argument that one expects a roughly constant star formation rate per unit line luminosity for high density tracers (e.g., HCN), and a star formation rate per unit luminosity that rises like luminosity to the ~ 0.5 for low density tracers (e.g., CO). However, in large surveys one cannot always determine the mean density in a galaxy, which would be required to construct an observational analog to Figure 2. Instead, we can use our calculated dependence of star formation rate and line luminosity on density to compare to observations as follows. Equation (9) gives the total molecular line luminosity per unit volume and equation (2) gives the star formation rate, which we convert to an IR luminosity via equation (11). For fixed assumed volume of molecular star-forming gas ($V_{\rm mol}$) we can then predict the expected correlations between L' in a given molecular line and $L_{\rm FIR}$. The three panels of Figure 3 show our results for $L_{\rm FIR}$ as a function of $L'_{\rm CO}$, $L'_{\rm HCN}$, and $L'_{\rm HCO^+}$ for the intermediate model (see Table 1) and for several values of $V_{\rm mol}$. Figure 4 shows how are results vary as a function of the assumed T and $\mathcal{M}$. There, for fixed $V_{\rm mol}$, we compare our predictions for the intermediate model with the normal and starburst models. In both figures we compare our models to data culled from the literature.

From the work of Gao & Solomon (2004a,b), Greve et al. (2005, their Fig. 7), Riechers et al. (2006b, their Fig. 5), and Gao et al. (2007), as well as the theoretical arguments in the preceding sections, we expect a strong, but not linear, correlation between the CO luminosity and the star formation rate — as measured by $L_{\rm FIR}$ — with the approximate form $L_{\rm FIR} \propto L'^{3/2}_{\rm CO}$. The left panel of Figure 3 shows the CO data, the approximate correlation expected (*solid line segment*; offset from the data for clarity) and the theoretical prediction (*solid lines*) for a total volume of molecular gas of $V_{\rm mol} = 10^7$, 10^8, and 10^9 pc^3. Because at fixed $L_{\rm FIR}$, galaxies exhibit a dispersion in $V_{\rm mol}$ we expect there to be intrinsic scatter in this correlation, roughly bracketed by the range of $V_{\rm mol}$ plotted.

The middle and right panels of Figure 3 show the same prediction for $L'_{\rm HCO^+}$ and $L'_{\rm HCN}$. In these cases, because the molecular line luminosity is nearly linearly proportional to $L_{\rm FIR}$, the dependence on $V_{\rm mol}$ is much weaker than for $L'_{\rm CO}$. However, systematic changes or differences in the fiducial parameters for the calculation (see Table 1) introduce uncertainty and scatter into the correlation. Figure 4 assesses this dependence. It compares the predictions of our model for normal (*dot-dashed lines*), intermediate (*solid lines*), and starburst (*dashed lines*) galaxies, as defined in Table 1, for fixed $V_{\rm mol} = 10^8$ pc^3. Our simple model reproduces the data rather well, and it predicts that generically there may be more intrinsic scatter in the $L'_{\rm CO} - L_{\rm FIR}$ correlation than in either $L'_{\rm HCN} - L_{\rm FIR}$ or $L'_{\rm HCO^+} - L_{\rm FIR}$.

Note that in both the middle and right panels of Figures 3 and 4, one expects a turn upward in the correlation at high $L_{\rm FIR}$, a deviation from linearity. This follows from the fact that in our model, at fixed $V_{\rm mol}$, systems with higher $L_{\rm FIR}$ have higher average densities. At sufficiently high $L_{\rm FIR}$ we thus expect $L'_{\rm HCN} - L_{\rm FIR}$ and $L'_{\rm HCO^+} - L_{\rm FIR}$ to steepen, in analogy with the $L'_{\rm CO} - L_{\rm FIR}$

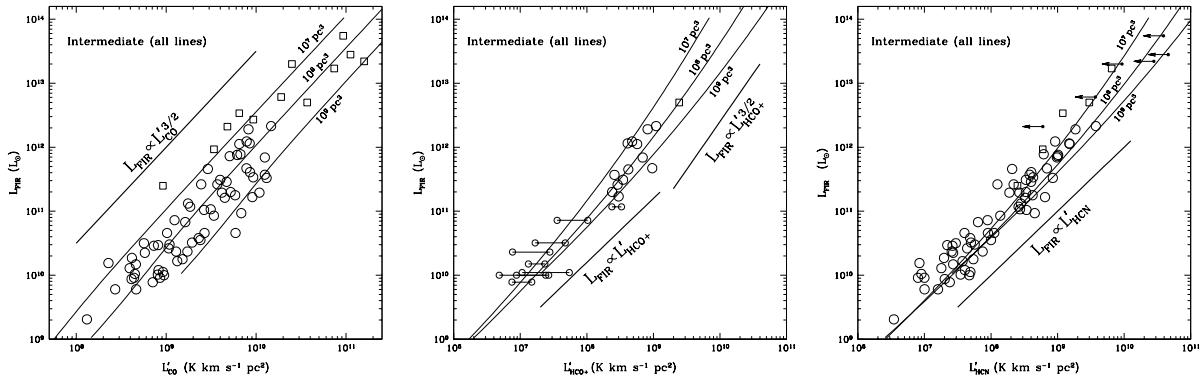

FIG. 3.— $L_{\rm FIR}$ ($L_\odot$) versus $L'_{\rm CO}(1\rightarrow0)$ (*left panel*), $L'_{\rm HCO^+}(1\rightarrow0)$ (*middle panel*), and $L'_{\rm HCN}(1\rightarrow0)$ (K km s^{-1} pc^2; *right panel*). The lines in each panel derive from the model presented in this paper with a constant total volume of molecular material of 10^7, 10^8, and 10^9 pc^3 (lowest to highest). The thick solid line segment shows power-law slopes to guide the eye. Data in the left and right panels are from Gao & Solomon (2004a,b) (*circles*) and Gao et al. (2007) (*open squares* for detections, *arrows* for upper limits). The middle panel combines data from Nguyen et al. (1992) (*small circles with lines*), Graciá-Carpio et al. (2006) (*big circles*), and Riechers et al. (2006b) (*open square*; using the Gao et al. (2007) FIR luminosity and magnification factor). For all data, $L_{\rm FIR}$ is defined based on a weighted sum of the galaxy luminosity in the 60 and 100 μm IRAS bands, as described by Sanders & Mirabel (1996). For the Nguyen et al. (1992) data, the uncertainties in $L_{\rm HCO^+}$ indicated by the lines arise because Nguyen et al. provide both HCN$(1\rightarrow0)$ and HCO$^+(1\rightarrow0)$ intensities, but the values for $L'_{\rm HCN}$ derived from their work generally fall a factor of $2-3$ below the $L'_{\rm HCN}$ from Gao & Solomon (2004a,b) for the same systems. This is probably because Nguyen et al. use a single beam pointing rather than integrating fully over extended sources, and therefore miss some of the flux. We therefore show two values of $L'_{\rm HCO^+}$, connected by a line, for each Nguyen et al. data point: a smaller value calculated directly from the data listed in their Table 2, and a larger value obtained by multiplying the $L'_{\rm HCN}$ value of Gao & Solomon for that galaxy by the ratio $I_{\rm HCO+}/I_{\rm HCN}$ measured by Nguyen et al. If this ratio is constant over the source, this estimate should correctly account for the flux outside the beam in the Nguyen et al. HCO$^+$ observation.

correlation. The data points with very high $L_{\rm FIR}$ in Figures 3 and 4, which might be used to test this prediction of our model, are gravitationally lensed, at high redshift, and contaminated by bright AGN. It is therefore unclear if the deviation from linearity implied particularly by the upper limits in $L'_{\rm HCN}$ in the right panels of Figures 3 and 4 is a result of enhanced $L_{\rm FIR}$, caused by the AGN emission (Carilli et al. 2005), or is instead a result of less molecular line emission per unit star formation, as our model implies (Fig. 2). Gao et al. (2007) note, however, that in the three systems for which the contribution from the AGN has been estimated (F10214+4724, D. Downes & P. Solomon 2007, in preparation; Cloverleaf, Weiß et al. 2003; APM 08279+5255, Weiß et al. 2005, 2007) the corrections are only significant for APM 08279+5255. This suggests that the data are so far consistent with our interpretation, but clearly much more data at high $L_{\rm FIR}$ — or, more precisely for our purposes, at high density — is required to test our predictions. We discuss the issue of AGN contamination further in § 4.3.

As a final note, the data so far *do* support the utility of HCO$^+$ as a useful tracer of dense gas. Papadopoulos (2007) has argued against the utility of HCO$^+$ as a faithful tracer of mass in starbursts on the basis that, since it is an ion, its abundance is strongly dependent on the free-electron abundance and might therefore vary strongly between galaxies with different ionizing radiation backgrounds. We cannot rule out this possibility given the limited data set available, but we see no strong evidence in favor of it from the data shown in Figures 3 and 4. As we have argued, HCO$^+(1\rightarrow0)$ is particularly useful because its critical density is between that of CO$(1\rightarrow0)$ and HCN$(1\rightarrow0)$ and, thus, as Figure 3 and 4 show, the correlation between $L_{\rm FIR}$ and $L'_{\rm HCO+}$ should steepen from linear to super-linear over the range of galaxies presented in the CO panels. A careful, large-scale HCO+$(1\rightarrow0)$ survey similar to the work of Gao & Solomon (2004a) on HCN$(1\rightarrow0)$ should reveal these trends. Lines with similarly low excitation temperatures and intermediate critical densities like CS$(1\rightarrow0)$ should behave analogously.

4. DISCUSSION

4.1. *Implications for Kennicutt-Schmidt Laws and Star Formation Efficiencies*

Our results suggest that KS laws in different tracers naturally fall into two regimes, although there is a broad range of molecular tracers that are intermediate between the two extremes. Tracers for which the critical density is small compared to the median density in a galaxy represent one limit. In these tracers, the light faithfully follows the mass, so the KS law measures a relationship between total mass and star formation. In any model in which star formation occurs at a roughly constant rate per dynamical time, this must produce a KS law in which the star formation rate rises with density to a power of near 1.5, and the ratio of star formation to luminosity rises as density to the 0.5 power. In terms of surface rather than volume densities, this implies $\dot{\Sigma}_* \propto \Sigma_g^{3/2} h^{-1/2}$. If we further add the observation that the scale heights h of the star-forming molecular layers of galaxies are roughly constant across galaxy types, one form of the observed Kennicutt (1998a,b) star formation law follows immediately (Elmegreen 2002). Moreover, in a galactic disk, $h \propto \Sigma_g/\overline{n}$ and $\overline{n} \propto \Omega^2/Q$ (e.g. Thompson et al. 2005); since in star-forming disks the Toomre-Q is about unity (Martin & Kennicutt 2001), substituting for h immediately gives $\dot{\Sigma}_* \propto \Sigma\Omega$, the alternate form of the Kennicutt (1998a,b) law.

The other limit is tracers for which the critical density is large compared to the median galactic density. These tracers pick out a particular density independent of the

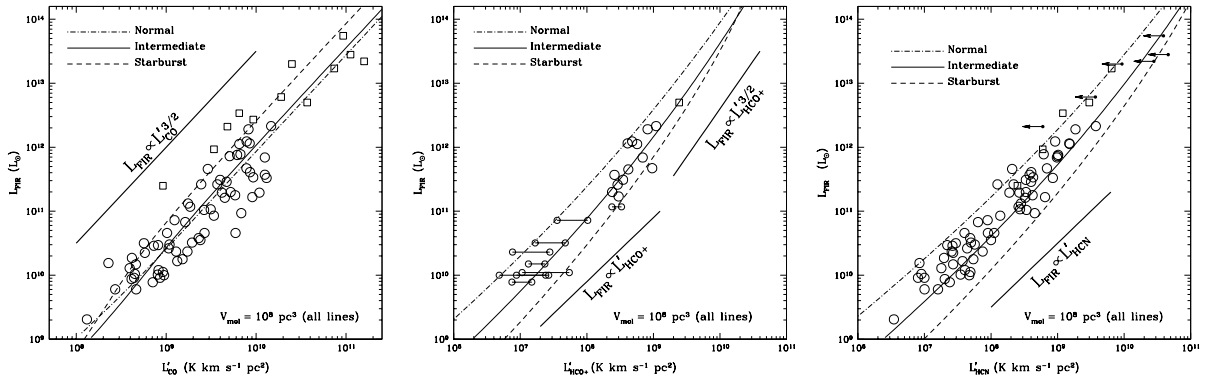

FIG. 4.— The same as Figure 3, but with constant $V_{\rm mol} = 10^8$ pc^3, and for the model parameters corresponding to "starburst" (*dashed*), "intermediate" (*solid*), and "normal" (*dot-dashed*) (see Table 1). Therefore, the middle solid line in each panel of Figure 3 is the same as the solid line in each panel in this Figure.

mean or median density in the galaxy, and thus all the regions they identify have the same dynamical time regardless of galactic environment. In this case the star formation rate will simply be proportional to the total mass of the observed regions, yielding a constant ratio of star formation rate to mass, as is observed for HCN in the local universe (Fig. 3, right panel; Gao & Solomon 2004a,b; Wu et al. 2005).

We predict that there should be a transition between linear and super-linear scaling of $L_{\rm FIR}$ with line luminosity at the point where galaxies transition from median densities that are smaller than the line critical density to median densities larger than the critical density. The $HCO^+(1 \rightarrow 0)$ line, and other lines with similar critical densities, e.g. $CS(1 \rightarrow 0)$ and $SO(1 \rightarrow 0)$, should show this behavior for galaxies in the local universe. The observed correlation between $L_{\rm HCO^+}$ and $L_{\rm FIR}$ appears to be consistent with our prediction, although at present the data are not of sufficient quality to distinguish between a break and a single powerlaw relation. There are hints that the very highest luminosity star-forming galaxies, which all reside at high redshift and may well reach ISM densities not found in any local systems, show such a break in the IR-HCN correlation.

One important point to emphasize in this analysis is that we have been able to explain the observed correlations between line and infrared luminosities, and hence between gas masses at various densities and star formation rates, without resorting to the hypothesis that the star formation process is fundamentally different in galaxies of different properties. Although uncertainties in both our model and the observations do not preclude an order-unity change in the star formation efficiency or $\rm SFR_{ff}$ as a function of $L_{\rm FIR}$, there is currently no evidence for such a change in the data, contrary to claims made by, e.g. Graciá-Carpio et al. (2006). In fact, all of the observational trends are predicted by our simple model with *constant* star formation efficiency. This is consistent with other lines of evidence that the fraction of mass at a given density that turns into stars is roughly 1% per free-fall time independent of density (Krumholz & Tan 2007).

4.2. *Does Star Formation Have a Fundamental Size or Density Scale?*

Based on the linear correlation between $HCN(1 \rightarrow 0)$ luminosity and star formation rate, seen both in external galaxies and in individual molecular clumps in the Milky Way, Gao & Solomon (2004a,b) and Wu et al. (2005) propose that $HCN(1 \rightarrow 0)$ emission traces a fundamental unit of star formation. They explain the linear IR-HCN correlation as a product of this; in their model, HCN luminosity correlates linearly with star formation rate because HCN luminosity simply counts the number of such units.

Based on our analysis, we argue that this hypothesis is only partially correct. We concur with Gao & Solomon and Wu et al. that the $HCN(1 \rightarrow 0)$ luminosity of a galaxy does simply reflect the mass of gas that is dense enough to excite the $HCN(1 \rightarrow 0)$ line. However, our analysis shows that this does not necessarily imply that this density represents a special density in the star formation process, or that objects traced by $HCN(1 \rightarrow 0)$ represent a physically distinct class. We show that a linear correlation between star formation rate and line luminosity is expected for any line with a critical density comparable to or larger than the median molecular cloud density in the galaxies used to define the correlation. It is possible that $HCN(1 \rightarrow 0)$-emitting regions represent a physically distinct scale of star formation as Wu et al. propose, but one can explain the linear IR-HCN correlation equally well if they are just part of the same continuous medium as the regions traced by $CO(1 \rightarrow 0)$ and by other transitions. Even the star-forming clouds themselves may simply be parts of a continuous distribution of ISM structures occupying the entire galaxy, as argued by Wada & Norman (2007). In this case there need be no special density scales other than the mean and median densities for the star-forming clouds on their largest scales, and the density at which star formation becomes rapid, converting the mass into stars in of order a free-fall time. This transition scale is unknown, but must be considerably larger than the density traced by HCN (Krumholz & Tan 2007).

4.3. *Limitations and Cautions*

4.3.1. *Self-Consistency*

As mentioned in § 3.2, our approach of leaving the gas temperature T and Mach number $\mathcal{M}$ as free parameters is not entirely consistent with our calculation of the

IR luminosity, since the IR luminosity and temperature are of course related. In principle, with a model of how the energy output from stars heats the dust and gas, together with a structural model connecting the energy and momentum output from stars to the generation of turbulence, it should be possible to self-consistently compute both the gas temperature and the Mach number from the volumetric star formation rate (see, e.g., Thompson et al. 2005). Such a model would return T and $\mathcal{M}$ as a function of $\overline{n}$ and possibly other galaxy properties, while simultaneously predicting a set of Kennicutt-Schmidt laws.

If the line luminosity depended strongly on T or $\mathcal{M}$, or if one required knowledge of the temperature to compute the infrared luminosity of a galaxy, we would would have no alternative to constructing such a model if we wished to explain the observed IR-line luminosity correlation. However, we can avoid this by relying on the observationally-calibrated star formation-IR correlation, and because, as we show in Figures 2, 3, and 4, the line luminosity varies quite weakly over a reasonable range of T and $\mathcal{M}$ for our chosen lines. For this reason, any model for computing T and $\mathcal{M}$ as a function of galaxy properties, if it were consistent with observations, would not significantly alter the IR-line luminosity correlation we derive. This is true, however, only for lines that require low temperatures to excite. As we discuss in § 4.3.2, lines that require higher temperatures to excite do depend sensitively on the temparature in the galaxy, and a model capable of predicting the IR-line luminosity correlation for these lines must also include a calculation of the temperature structure of the galaxy.

4.3.2. *Isothermality*

Our assumption of isothermality means that our analysis will only apply to molecular lines for which the temperature $T_{\rm up}$ corresponding to the upper state energy is < 10 K, low enough to be excited even in the coolest molecular clouds in normal spiral galaxies. The reason for this is that at temperatures larger than $T_{\rm up}$, the luminosity in a line generally varies at most linearly with the temperature. As the similarity between the results with our different galaxy models illustrates, changing the temperature within the range of $\sim 10 - 50$ K produces only a factor of a few change in the luminosity of the lines we have studied. In contrast, line luminosity responds exponentially to temperature changes when the temperature is below the value corresponding to the upper state's energy. This means that lines sensitive to high temperatures pick out primarily the regions that are warm enough for the line to be excited. Density has only a secondary effect. The emission will therefore reflect the temperature distribution in star-forming clouds more than the density distribution, an effect that our isothermal assumption precludes us from treating. KS laws in high temperature tracers are likely to find linear relationships between star formation rate and mass regardless of the critical density of the molecule in question because they will simply be correlating the mass of dust warmed to $\gtrsim 100$ Kelvin, which is essentially what is measured by $L_{\rm FIR}$, with the mass of gas warmed to temperatures above $T_{\rm up}$. However, our model will not apply to these lines, and for this reason we do not attempt to compare to observations using higher transitions of CO ($3 \rightarrow 2$, $4 \rightarrow 3$, $5 \rightarrow 4$, $6 \rightarrow 5$, and $7 \rightarrow 6$, which have $T_{\rm up} = 33, 55, 83, 116$, and 154 K, respectively; Greve et al. 2005, Solomon & Vanden Bout 2005), CS($5 \rightarrow 4$) ($T_{\rm up} = 35$ K; Plume et al. 1997), or other high temperature tracers.

4.3.3. *Molecular Abundances*

We have not considered density-dependent variations in molecule abundances. One potential source of variation in molecular abundance is freeze-out onto grain surfaces at high densities and low temperatures (e.g. Tafalla et al. 2004a,b). Chemodynamical models suggest that freeze-out is not likely to become significant for either carbonaceous or nitrogenous species until densities $n \gtrsim 10^6$ cm^{-3} (Flower et al. 2006), but may become severe at higher densities, so whether depletion is significant depends on what fraction of the total luminosity would be contributed by gas of this density or higher were there no freeze-out. Figure 1 suggests that freeze-out is likely to modify the total galactic luminosity of CO, HCO$^+$, and HCN fairly little even at a mean ISM density of $\overline{n} = 10^4$ cm^{-3}, but may have significant effects for galaxies of larger mean densities or for lines for which the critical densities is comparable to the freeze-out density. If freeze-out is significant, our conclusions will be modified.

4.3.4. *Atomic Gas*

In the simple model developed here, we have neglected the role of atomic gas entirely. Whether the density or surface density of atomic gas plays a role in controlling the star formation rate is subject to debate on both observational and theoretical grounds (Kennicutt 1998a,b; Wong & Blitz 2002; Heyer et al. 2004; Komugi et al. 2005; Krumholz & McKee 2005; Kennicutt et al. 2007), so it is unclear how much a limitation this omission really is. We can say with confidence that in molecule-rich galaxies, which provide almost all the dynamic range of both the Kennicutt (1998a,b) correlation and the correlations illustrated in Figures 3 and 4, the atomic gas plays almost no role simply because there is so little of it. Thus, our predictions should be quite robust, except perhaps at the very low luminosity ends of Figures 3 and 4.

4.3.5. *AGN Contributions*

A final point is not so much a limitation of our work as a cautionary note about comparing our model with observations. We have included in our model IR luminosity only from star formation, and molecular line luminosity only from molecules in cold star-forming clouds. However, an AGN may make a significant contribution to a galaxy's luminosity in the far infrared by direct heating of dust grains, and in molecular lines via an X-ray dissociation region. Indeed, several of the systems with the highest IR luminosities in Figures 3 and 4 are contaminated by AGN. As noted in §3.3, this complicates an assessment of our prediction of an up-turn in the $L'_{\rm HCN} - L_{\rm FIR}$ and $L'_{\rm HCO+} - L_{\rm FIR}$ correlations at high luminosity. This deviation from linearity at high gas density (at fixed $V_{\rm mol}$, high $L_{\rm FIR}$) is an essential prediction of our model, but testing it relies on a careful separation of the contribution of the AGN to both the IR and line luminosities (e.g. Maloney et al. 1996). In fact, Carilli et al. (2005) discuss

the possibility that the AGN's contribution to the IR luminosity in these systems causes them to be above the local linear $L'_{\rm HCN} - L_{\rm FIR}$ correlation. Such a contamination would mimic the prediction of our model. However, Gao et al. (2007) argue that the sub-millimeter galaxies in their sample are not AGN dominated and that just one of three quasars in their sample (APM 08279+5255) has a large AGN IR component. See Gao et al. (2007) for more discussion. For these reasons we contend that although our model is consistent with the existing data, the current evidence for a break in the $L'_{\rm HCN} - L_{\rm FIR}$ correlation should be viewed with caution and more data in high density/luminosity systems is clearly required to understand the role of AGN contamination in shaping the correlation.

5. CONCLUSIONS

We provide a simple model for understanding how Kennicutt-Schmidt laws, which relate the star formation rate to the mass or surface density of gas as inferred from some particular line, depend on the line chosen to define the correlation. We show that for a turbulent medium the luminosity per unit volume in a given line, provided that line can be excited at temperatures lower than the mean temperature in a galaxy's molecular clouds, increases faster than linearly with the density for molecules with critical densities larger than the median gas density. The star formation rate also rises super-linearly with the gas density, and the combination of these two effects produces a close to linear correlation between star formation rate and line luminosity. In contrast, the line luminosity rises only linearly with density for lines with low critical densities, producing a correlation between star formation rate and line luminosity that is super-linear.

Based on this analysis, we construct a model for the correlation between a galaxy's infrared luminosity and its luminosity in a particular molecular line. Our model is extremely simple, in that it relies on an observationally-calibrated IR-star formation rate correlation, it treats molecular clouds as having homogenous density and velocity distributions, temperatures, and chemical compositions, and it only very crudely accounts for variations in molecular cloud properties across galaxies. Despite these approximations, the model naturally explains why some observed correlations between infrared luminosity and line luminosity in galaxies are linear, and some are super-linear. Using it, we are able to compute quantitatively the correlation between infrared and HCN($1 \rightarrow 0$) line luminosity, and between IR and CO($1 \rightarrow 0$) line luminosity. We show that our model provides a very good fit to observations in these lines, and we are able to make similar predictions for any molecular line that can be excited at low temperatures, as we demonstrate for the example of $HCO^+(1 \rightarrow 0)$. Moreover, we are able to explain the observed data without recourse to the hypothesis that the star formation process is somehow different, either more or less efficient, in different types of galaxies or for media of different densities. Instead, our model is able to explain the observed correlations using a simple, universal star formation law.

One strong prediction of our model is that there should be a break from linear to non-linear scaling in the HCN-IR correlation at very high IR luminosity, and a similar break in the HCO^+-IR correlation at somewhat lower luminosity. The data for HCO^+ are consistent with this prediction but do not yet strongly favor a break over pure powerlaw behavior. However, there is some preliminary evidence for a break in the IR-HCN correlation in high redshift galaxies more luminous than any found in the local universe, although with these high redshift observations it is difficult to rule out the alternative explanation of the break as arising due to a progressively rising AGN contribution to the IR luminosity (see §3.3 and §4.3.5). Future galaxy surveys both in the local universe and at high redshift may be used to test our predictions for $HCO^+(1 \rightarrow 0)$, HCN($1 \rightarrow 0$), and other molecular lines.

We thank L. Blitz, B. Draine, A. Leroy, E. Rosolowsky, and A. Socrates for helpful discussions, N. Evans and the anonymous referee for useful comments on the manuscript, and R. Kennicutt for kindly providing a preprint of his submitted paper. We thank Y. Gao for providing $L_{\rm FIR}$ for the systems used in Figures 3 and 4. MRK acknowledges support from NASA through Hubble Fellowship grant #HSF-HF-01186 awarded by the Space Telescope Science Institute, which is operated by the Association of Universities for Research in Astronomy, Inc., for NASA, under contract NAS 5-26555. TAT acknowledges support from a Lyman Spitzer, Jr. Fellowship.

REFERENCES

Bell, E. F. 2003, ApJ, 586, 794
Black, J. H. 2000, in Astronomy, physics and chemistry of H_3^+, 2515
Calzetti, D., Armus, L., Bohlin, R. C., Kinney, A. L., Koornneef, J., & Storchi-Bergmann, T. 2000, ApJ, 533, 682
Carilli, C. L., Solomon, P., Vanden Bout, P., Walter, F., Beelen, A., Cox, P., Bertoldi, F., Menten, K. M., Isaak, K. G., Chandler, C. J., & Omont, A. 2005, ApJ, 618, 586
Combes, F. 1991, ARA&A, 29, 195
Dale, D. A., Helou, G., Contursi, A., Silbermann, N. A., & Kolhatkar, S. 2001, ApJ, 549, 215
Downes, D. & Solomon, P. M. 1998, ApJ, 507, 615
Elmegreen, B. G. 1994, ApJ, 425, L73
—. 2002, ApJ, 577, 206
Elmegreen, B. G. & Scalo, J. 2004, ARA&A, 42, 211
Flower, D. R., Pineau Des Forêts, G., & Walmsley, C. M. 2006, A&A, 456, 215
Gao, Y., Carilli, C. L., Solomon, P. M., & Vanden Bout, P. A. 2007, ApJ, in press, astro-ph/0703548
Gao, Y. & Solomon, P. M. 2004a, ApJS, 152, 63
—. 2004b, ApJ, 606, 271
Graciá-Carpio, J., García-Burillo, S., Planesas, P., & Colina, L. 2006, ApJ, 640, L135
Greve, T. R., Bertoldi, F., Smail, I., Neri, R., Chapman, S. C., Blain, A. W., Ivison, R. J., Genzel, R., Omont, A., Cox, P., Tacconi, L., & Kneib, J.-P. 2005, MNRAS, 359, 1165
Heyer, M. H., Corbelli, E., Schneider, S. E., & Young, J. S. 2004, ApJ, 602, 723
Hirashita, H., Buat, V., & Inoue, A. K. 2003, A&A, 410, 83
Iglesias-Páramo, J., Buat, V., Takeuchi, T. T., Xu, K., Boissier, S., Boselli, A., Burgarella, D., Madore, B. F., Gil de Paz, A., Bianchi, L., Barlow, T. A., Byun, Y.-I., Donas, J., Forster, K., Friedman, P. G., Heckman, T. M., Jelinski, P. N., Lee, Y.-W., Malina, R. F., Martin, D. C., Milliard, B., Morrissey, P. F., Neff, S. G., Rich, R. M., Schiminovich, D., Seibert, M., Siegmund, O. H. W., Small, T., Szalay, A. S., Welsh, B. Y., & Wyder, T. K. 2006, ApJS, 164, 38
Juvela, M., Padoan, P., & Nordlund, Å. 2001, ApJ, 563, 853
Kennicutt, R. C. 1998a, ARA&A, 36, 189

—. 1998b, ApJ, 498, 541
Kennicutt, R. C., Calzetti, D., Walter, F., Helou, G., Hollenbach, D. J., Armus, L., Bendo, G., Dale, D. A., Draine, B. T., Engelbracht, C. W., Gordon, K. D., Prescott, M. K. M., Regan, M. W., Thornley, M. D., Bot, C., Brinks, E., de Blok, E., de Mello, D., Meyer, M., Moustakas, J., Murphy, E. J., Sheth, K., & Smith, J. D. T. 2007, ApJ, submitted
Komugi, S., Sofue, Y., Nakanishi, H., Onodera, S., & Egusa, F. 2005, PASJ, 57, 733
Krumholz, M. R. & McKee, C. F. 2005, ApJ, 630, 250
Krumholz, M. R. & Tan, J. C. 2007, ApJ, 654, 304
Lahuis, F. & van Dishoeck, E. F. 2000, A&A, 355, 699
Mac Low, M. & Klessen, R. S. 2004, Reviews of Modern Physics, 76, 125
Madore, B. F. 1977, MNRAS, 178, 1
Maloney, P. R., Hollenbach, D. J., & Tielens, A. G. G. M. 1996, ApJ, 466, 561
Martin, C. L. & Kennicutt, R. C. 2001, ApJ, 555, 301
McKee, C. F. 1999, in NATO ASIC Proc. 540: The Origin of Stars and Planetary Systems, 29
Netzer, H., Lemze, D., Kaspi, S., George, I. M., Turner, T. J., Lutz, D., Boller, T., & Chelouche, D. 2005, ApJ, 629, 739
Neufeld, D. A., Melnick, G. J., Sonnentrucker, P., Bergin, E. A., Green, J. D., Kim, K. H., Watson, D. M., Forrest, W. J., & Pipher, J. L. 2006, ApJ, 649, 816
Nguyen, Q.-R., Jackson, J. M., Henkel, C., Truong, B., & Mauersberger, R. 1992, ApJ, 399, 521
Nordlund, Å. K. & Padoan, P. 1999, in Interstellar Turbulence, 218
Ostriker, E. C., Gammie, C. F., & Stone, J. M. 1999, ApJ, 513, 259
Padoan, P. & Nordlund, Å. 2002, ApJ, 576, 870
Papadopoulos, P. P. 2007, ApJ, 656, 792
Plume, R., Jaffe, D. T., Evans, N. J., Martin-Pintado, J., & Gomez-Gonzalez, J. 1997, ApJ, 476, 730
Riechers, D. A., Walter, F., Carilli, C. L., Knudsen, K. K., Lo, K. Y., Benford, D. J., Staguhn, J. G., Hunter, T. R., Bertoldi, F., Henkel, C., Menten, K. M., Weiss, A., Yun, M. S., & Scoville, N. Z. 2006a, ApJ, 650, 604
Riechers, D. A., Walter, F., Carilli, C. L., Weiss, A., Bertoldi, F., Menten, K. M., Knudsen, K. K., & Cox, P. 2006b, ApJ, 645, L13
Rowan-Robinson, M., Mann, R. G., Oliver, S. J., Efstathiou, A., Eaton, N., Goldschmidt, P., Mobasher, B., Serjeant, S. B. G., Sumner, T. J., Danese, L., Elbaz, D., Franceschini, A., Egami, E., Kontizas, M., Lawrence, A., McMahon, R., Norgaard-Nielsen, H. U., Perez-Fournon, I., & Gonzalez-Serrano, J. I. 1997, MNRAS, 289, 490
Sanders, D. B. & Mirabel, I. F. 1996, ARA&A, 34, 749
Schmidt, M. 1959, ApJ, 129, 243
—. 1963, ApJ, 137, 758
Schöier, F. L., van der Tak, F. F. S., van Dishoeck, E. F., & Black, J. H. 2005, A&A, 432, 369
Solomon, P. M., Downes, D., Radford, S. J. E., & Barrett, J. W. 1997, ApJ, 478, 144
Solomon, P. M., Rivolo, A. R., Barrett, J., & Yahil, A. 1987, ApJ, 319, 730
Solomon, P. M. & Vanden Bout, P. A. 2005, ARA&A, 43, 677
Tafalla, M., Myers, P. C., Caselli, P., & Walmsley, C. M. 2004a, A&A, 416, 191
—. 2004b, Ap&SS, 292, 347
Thompson, T. A., Quataert, E., & Murray, N. 2005, ApJ, 630, 167
Wada, K. & Norman, C. 2007, ApJ, in press, astro-ph/0701595
Weiß, A., Downes, D., Neri, R., Walter, F., Henkel, C., Wilner, D. J., Wagg, J., & Wiklind, T. 2007, A&A, 467, 955
Weiß, A., Downes, D., Walter, F., & Henkel, C. 2005, A&A, 440, L45
Weiß, A., Henkel, C., Downes, D., & Walter, F. 2003, A&A, 409, L41
Wild, W., Harris, A. I., Eckart, A., Genzel, R., Graf, U. U., Jackson, J. M., Russell, A. P. G., & Stutzki, J. 1992, A&A, 265, 447
Wong, T. & Blitz, L. 2002, ApJ, 569, 157
Wu, J., Evans, N. J., Gao, Y., Solomon, P. M., Shirley, Y. L., & Vanden Bout, P. A. 2005, ApJ, 635, L173
Yao, L., Seaquist, E. R., Kuno, N., & Dunne, L. 2003, ApJ, 588, 771
Zaritsky, D., Kennicutt, Jr., R. C., & Huchra, J. P. 1994, ApJ, 420, 87